2017 IEEE First Ukraine Conference on Electrical and Computer Engineering (UKRCON)

Mathematical Model of Volume Optical Interconnection Reconfiguration Utilizing Acousto-Optic Beam Forming

V.S. Tkachenko
Radiophysics and Cybersecurity Department
Vasyl' Stus Donetsk National University
600-richya str. 21, 21021, Vinnytsia, Ukraine
tkachenko_vera@i.ua

A.Y. Lipinskii
Electronics Department
National Aviation University
Prospect Komarova 1, 03058, Kiev, Ukraine
lipinskii@nau.edu.ua

***Abstract* —The mathematical model of volume optical interconnection reconfiguration by acousto-optical beam forming approach is proposed in the paper. The restrictions of proposed model were considered as well as results of simulations of interconnections' patterns were presented.**

Keywords — Acousto-optic; computing environment; photorefractive media

I. INTRODUCTION

Optical computing systems have a great potential to solve many problems of modern computing and signal processing applications [1-3]. Restriction in quantity of interconnections on semiconductor integrated circuits can be solved by the creation of volume optical interconnections and incoherent optical computing devices [4] as the next step.

The optoelectronic acousto-optical computing environment (OACE) [5] with memory cells based on a reversible photorefractive storage medium (RPSM) is an analog of programmable logic integrated devices (PLD) because of its architecture.

Architecture configuration of the computing device based on PLD is done by programming of relevant connections between logic blocks of a crystal. It is possible to use the analogy of PLD and OACE for describing the diffraction gratings record which present configuration of volume interconnections in RPSM as a dynamical changing of OACE architecture.

The mathematical model of volume interconnections' reconfiguration for dynamical changes of OACE functions is proposed in this paper. The considered reconfiguration apparatus includes the acousto-optic beam-forming devices. The restrictions of proposed model were analyzed.

II. DYNAMICAL CHANGING OF OACE ARCHITECTURE BY RECONFIGURATION OF VOLUME INTERCONNECTIONS

Electronic computing systems with optical functional blocks that increase their performance were described in [7-9]. Furthermore, a reconfiguration of connections between the logic gates is permitted due to overwriting of a static hologram for VLSI circuits as reported in [8].

Volume interconnection structure in form of multichannel deflector matrix formed on RPSM is possible in OACE [10]. An information recording device contains two pairs of acousto-optical modulators working on the principle of parallel diffraction in the orthogonal acoustic beams [6]. In such scheme structure of high-performance optoelectronic computing (HPOC) module described in [4] is realized with advantage property – reconfiguration of OACE can be done dynamically instead of using of the static hologram.

Fig. 1 shows the OACE with dynamically reconfigurable architecture. It consists of two layers. The first layer performs a Boolean tensor product of paraphase input signals to generate a set of minterms specified by interconnection configuration correspondingly to the principle of duality, according to which the negation of logical sum of variables is a product of their negations. In this case, the result of the logical addition of the input signals received from the matrix of surface-emitting lasers with the vertical resonator (VCSEL) and redirected by a multi-channel matrix of RPSM deflector signals is formed on the selected element of the matrix of photodetectors and an interpreted as the corresponding minterm.

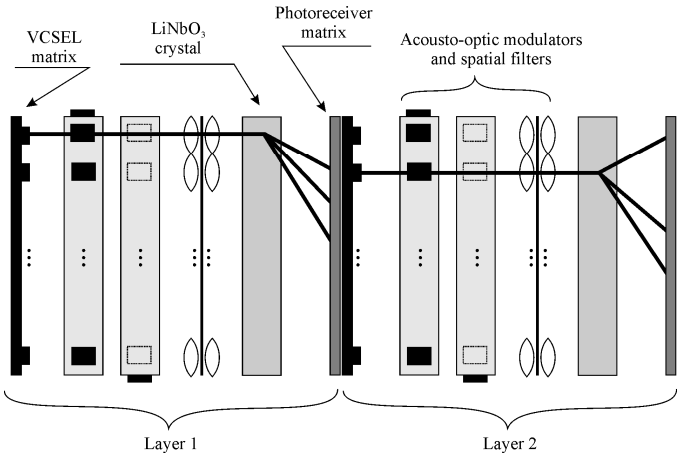

Fig. 1. Optoelectronic acousto-optic computing environment with dynamically reconfigurable architecture

978-1-5090-3006-4/17/$31.00 ©2017 IEEE

The next block implements the Boolean tensor addition of minterms of the first block generating a sum of the products in accordance with Shannon's generalized theorem of digital computation.

III. Mathematical Model Of Volume Optical Interconnections Reconfiguration

Let us consider system of acousto-optical modulators (layers 1, 2 in OACE, see fig.1) which uses scheme of parallel diffraction in orthogonal acoustic beams (Fig.2)

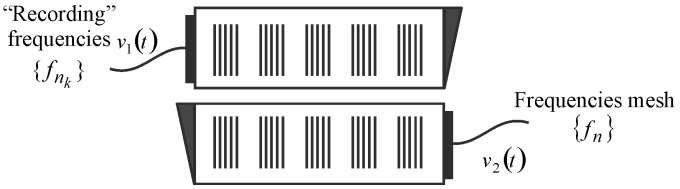

Fig. 2. Parallel diffraction in orthogonal acoustic beams scheme

It was shown in work [11] that with the axial lenses and the diaphragm forming the spatial filter that excludes 0-th order peek of diffraction, the intensity of the output optical beam $I_{out}(x,t)$ is given by the next relation:

$$I_{out}(x,t)=\left|j\frac{1}{2}\tilde{v}_1(t-x/V)+j\frac{1}{2}\tilde{v}_2(t+x/V-T)\right|^2 \qquad (1)$$

where V - sound velocity in a modulator medium, $T=W/V$ - a time of acoustic wave propagation in a cell with a length W, $\tilde{v}_1(t)$ and $\tilde{v}_2(t)$ - analytical signals, that correspond to electrical signals $v_1(t)$ and $v_2(t)$. Relation (1) may be modified for the simplification of further analysis [12]:

$$I_{out}(x,t)=\left(\frac{1}{4}\right)\left|\tilde{v}_1(t-x/V)\right|^2+\left(\frac{1}{4}\right)\left|\tilde{v}_2(t+x/V-T)\right|^2+ \\ +\left(\frac{1}{2}\right)\mathrm{Re}\left\{\tilde{v}_1^*(t-x/V)\tilde{v}_2(t+x/V-T)\right\} \qquad (2)$$

The first and the second terms in (2) become constant values [12] after integration within enough time interval. The third term may describe some spatial intensity distribution in dependence on carrier frequencies $\tilde{v}_1(t)$ and $\tilde{v}_2(t)$ as well as frequencies of modulating signals.

Let us consider two signals $v_1(t)$ and $v_2(t)$ that are described as follows:

$$v_1(t)=b_1(t)\cos(2\pi f_0 t),\ v_2(t)=b_2(t)\cos(2\pi f_0 t),$$

where $b_1(t)$ and $b_2(t)$ are modulating signals, f_0 is carrier frequency. Corresponding analytical signals may be written in the next form:

$$\tilde{v}_1(t)=b_1(t)\exp(j2\pi f_0 t),\quad \tilde{v}_2(t)=b_2(t)\exp(j2\pi f_0 t).$$

One may obtain for the third term (2):

$$(1/2)\mathrm{Re}\left\{\tilde{v}_1^*(t-x/V)\tilde{v}_2(t+x/V-T)\right\}= \\ (1/2)\mathrm{Re}\left\{b_1^*(t-x/V)b_2(t+x/V-T)\exp\left[i2\pi f_0\left(\frac{2x}{V}-T\right)\right]\right\}. \qquad (3)$$

Relation (3) will have the next form for the choice of $b_1(t)=b_2(t)=A$, here A is some constant value:

$$(1/2)\mathrm{Re}\left\{\tilde{v}_1^*(t-x/V)\tilde{v}_2(t+x/V-T)\right\}= \\ =1/2\,A^2\cos[2\pi f_0(2x/V-T)]$$

Intensity distribution $I_{out}(x,t)$ in this case is

$$I_{out}(x,t)=I_t(x,t)+\frac{1}{2}A^2\cos\left[2\pi f_0\left(\frac{2x}{V}-T\right)\right], \qquad (4)$$

where $I_t(x,t)$ is a time-dependent component of intensity which contains sum of time-dependent terms in $I_{out}(x,t)$.

As it was shown in [11] phase light modulator is formed by illuminating of $LiNbO_3$ by the light beam with the spatial distribution of intensity. According to (4), this phase light modulator may be described as a grating with a sinusoidal profile. The period is equal to a half of acoustic wavelength at the f_0 frequency.

Let's suppose that multicarrier signal with components f_1, f_2, …, f_N is on one of the optical modulators (fig.2). Components f_1, f_2, …, f_N form a frequency grid $\{f_n\}$. Then one has a signal with only a few frequencies from a grid $\{f_n\}$ of on the other acousto-optic modulator, e.g. f_{n_1}, f_{n_2}, …, f_{n_K} ($K \le N$) and frequency grid $\{f_{n_k}\}$. In this case, relations for $v_1(t)$ and $v_2(t)$ will be

$$v_1(t)=A\sum_{k=1}^{K}\cos(2\pi f_{n_k}t),\quad v_2(t)=A\sum_{n=1}^{N}\cos(2\pi f_n t).$$

Corresponding analytical signals $v_1(t)$ and $v_2(t)$ have form

$$\tilde{v}_1(t)=A\sum_{k=1}^{K}\exp(j2\pi f_{n_k}t),\quad \tilde{v}_2(t)=A\sum_{n=1}^{N}\exp(j2\pi f_n t).$$

The third term in (2) will be equal to

$$\left(\frac{1}{2}\right)\mathrm{Re}\left\{\tilde{v}_1^*(t-x/V)\tilde{v}_2(t+x/V-T)\right\}= \\ =\frac{A^2}{2}\mathrm{Re}\left\{\sum_{k=1}^{K}\sum_{n=1}^{N}\exp\left[j2\pi\left\{(f_n-f_{n_k})t+(f_n+f_{n_k})\frac{x}{V}-f_nT\right\}\right]\right\}= \\ =\sum I_{n_k=n}+\sum I_{n_k\neq n},$$

where $\sum I_{n_k=n}$ is a sum of intensities of components with the same frequencies $f_{n_k} = f_n$:

$$\sum I_{n_k=n} = \frac{1}{2} A^2 \sum_{k=1}^{K} \cos\left[2\pi f_{n_k} \left(\frac{2x}{V} - T \right) \right],$$

$\sum I_{n_k \neq n}$ is a sum of intensities with not equal f_{n_k} and f_n. This sum depends on time:

$$\sum I_{n_k \neq n} = \frac{A^2}{2} \times$$

$$\times \sum_{k=1}^{K} \sum_{n=1}^{N} \begin{cases} \cos\left[2\pi \left\{ \left(f_n - f_{n_k} \right) t + \left(f_n + f_{n_k} \right) \frac{x}{V} - f_n T \right\} \right], & n_k \neq n, \\ 0, & n_k = n. \end{cases}$$

Thus for multicarrier signals $v_1(t)$ and $v_2(t)$ intensity $I_{out}(x,t)$ is

$$I_{out}(x,t) = I_t(x,t) + \frac{1}{2} A^2 \sum_{k=1}^{K} \cos\left[2\pi f_{n_k} \left(\frac{2x}{V} - T \right) \right]. \quad (5)$$

The results of the spatial distribution of output light beam intensity modulation are shown the fig.3-5. Results are obtained for the functional model in Simulink package. Results for four carrier signal $v_2(t)$ and one carrier $v_1(t)$ is in fig.3. Fig.4 corresponds to two carrier signal $v_1(t)$. The case of three carrier signal $v_1(t)$ is in fig.5.

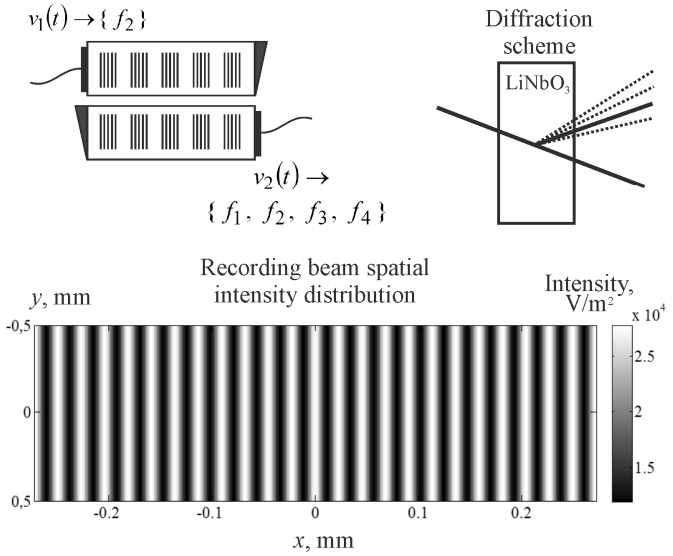

Fig. 3. Simulation results appropriate to four-carrier signal $v_2(t)$ and one carrier $v_1(t)$

As it can be seen for the figures, the resulting intensity distribution can be given with a help of proper choice of frequency components in $v_1(t)$ the signal. Thereby one can select the desired configuration of optical interconnections in RPSM for each block of OACE. Schemes from fig.3-5 correspond to the realization of one (fig.3), two (fig.4) and three (fig.5) interconnections depending on components of the signal $v_1(t)$.

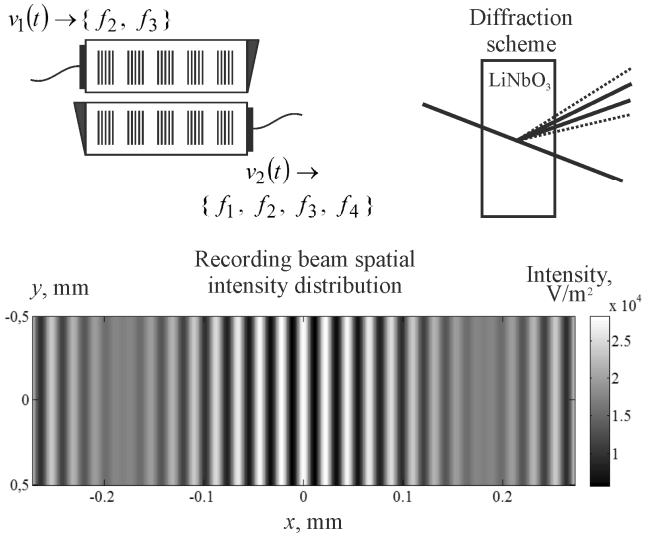

Fig. 4. Simulation results appropriate to four-carrier signal $v_2(t)$ and two-carrier $v_1(t)$

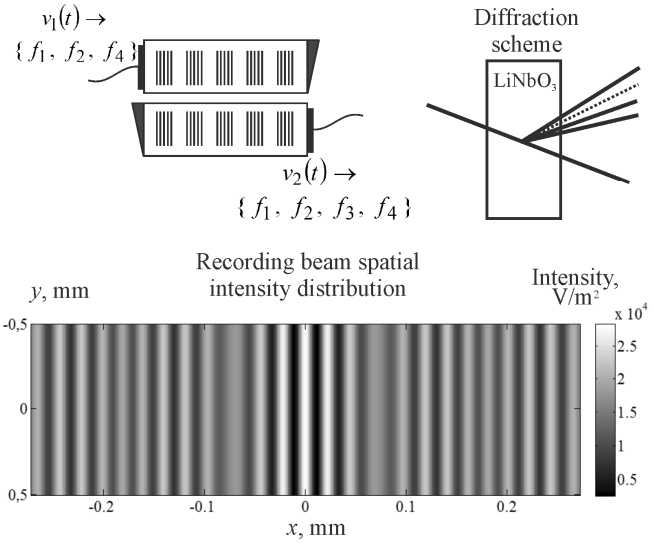

Fig. 5. Simulation results appropriate to four-carrier signal $v_2(t)$ and three-carrier $v_1(t)$

IV. Model Restrictions

Let us analyze the intensity of an output beam $I_{out}(x,t)$ for components with not equal frequencies in order to determine the allowable frequency instability of signal $v_1(t)$ and $v_2(t)$ generators as well as to find frequency resolution of the device. The expressions for analytical signals $\tilde{v}_1(t)$ and $\tilde{v}_2(t)$ may be written as

$$\tilde{v}_1(t) = A \exp\{ j 2\pi f_0 t \}, \quad \tilde{v}_2(t) = A \exp\{ j 2\pi (f_0 + \Delta f) t \},$$

where Δf is a difference of frequencies for $v_1(t)$ and $v_2(t)$. The third term in (2) is:

$$\left(\frac{1}{2}\right)\mathrm{Re}\left\{\tilde{v}_1^*(t-x/V)\tilde{v}_2(t+x/V-T)\right\}=$$
$$=\left(\frac{1}{2}\right)\mathrm{Re}\left\{A^2\exp\left[i2\pi\left\{\Delta f\cdot t+(2f_0+\Delta f)\frac{x}{V}-(f_0+\Delta f)T\right\}\right]\right\}= \quad (6)$$
$$=\frac{1}{2}A^2\cos\left[2\pi\left\{\Delta f\cdot t+(2f_0+\Delta f)\frac{x}{V}-(f_0+\Delta f)T\right\}\right].$$

Taking into account (6), the intensity of output optical beam can be written as follows:

$$I_{out}(x,t)=$$
$$=I_t(x,t)+\frac{1}{2}A^2\cos\left[2\pi\left\{\begin{array}{l}\Delta f\cdot t+(2f_0+\Delta f)\frac{x}{V}-\\-(f_0+\Delta f)T\end{array}\right\}\right] \quad (7)$$

The second term in this formula is spatial sinusoidal distribution moving with velocity $V_{\Delta f}$:

$$V_{\Delta f}=\frac{\Delta f}{2f_0+\Delta f}V. \quad (8)$$

Relation (8) is equal to zero for $\Delta f=0$ while formula (7) is equal to (4) for such case.

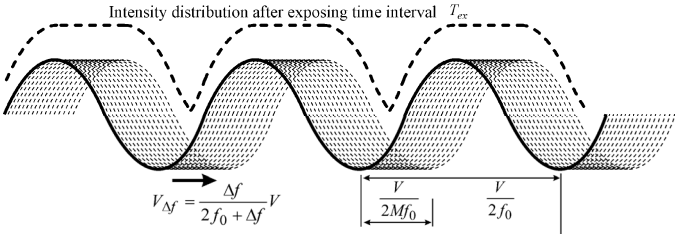

Fig. 6. Illustration of pattern displacement during writing influence on the grating contrasts

One needs to require that the pattern of intensity is displaced no more that on $1/M$ -part of recorded diffraction grating period (Fig.6), i.e. no more than $1/(2M)$ of an acoustic wavelength at the frequency f_0 during an exposure time T_{ex} to determine the allowable frequency instability.

Then, considering (8) Δf should satisfy the following inequality:

$$\Delta f\le\frac{2f_0}{2Mf_0T_{ex}-1}. \quad (9)$$

The f_h frequency resolution is determined by the condition of difference for adjacent channels. This difference needs to provide mutual illumination even for frequency instability of generators. Thus, the pattern of intensity distribution is displaced more than on two periods of recorded grating during the exposure time T_{ex} , and f_h should satisfy to inequality $f_h\ge 2f_0/(f_0T_{ex}-1)$.

V. Conclusion

In modern FPGA each logical element can be directly connected with dozens of adjacent logic elements. Thus calculating a function of many variables would require the equivalent circuit consisting of many blocks. This leads to a lowering of circuit performance with taking into account time delay in each block and to inability to satisfy time parameters of the problem solved. Existing technology allows obtaining the total number of OACE channels up to 512^2 (512 on one side of the matrix). In this case, the use of volume interconnections implemented by PRSM allows OACE to perform the calculation of matching function with 250 thousand logical variables (1st block performs multiplication, the 2nd block performs addition).

References

[1] "Optical computing: Digital and Symbolic," Ed. R. Arrathoon, New York: Marcell Dekker Inc., 1989.

[2] P.A. Belov, V.G. Bespalov, V.N. Vasiliev [et al.], "Optical processors: achievements and novel ideas," Problems of coferent and nonlinear optics, SPbGU ITMO Press, 2006. (in Russian)

[3] A.Y. Lipinskii, A.N. Rudiakova, V.V. Danilov, "Acoustooptic Binary Coding Based on Space-Time Integration and Its Application to Ultrafast High-Resolution Digital-Analog Conversion," IEEE Photonics Technology Letters, vol. 20, no. 24, pp. 2087–2089, 2008.

[4] P.S. Guilfoyle, J.M. Hessenbruch, R.V. Stone, "Free-Space optical interconnects for high performance optoelectronic switching," IEEE Trans. Comput., vol. 31, pp. 69-75, 1998.

[5] A.Y. Lipinskii, A.N. Rudiakova, "Acousto-optic computing environment for stream data processing," Applied Optics, vol. 50, pp. 4917–4921, 2011.

[6] V.S. Tkachenko, A.Y. Lipinskii, "Mathematical model of volume optical interconnection in $LiNbO_3$ crystal," 2016 IEEE International Conference on Mathematical Methods in Electromagnetic Theory (MMET), Lviv, pp. 204-207, 2016.

[7] Seto D., Nakajima M., Watanabe M. Dynamic optically reconfigurable gate array very large-scale integration with partial reconfiguration capability // Applied Optics. – 2010. – vol. 49, no. 36. – P. 6986-6994.

[8] Y. Arakawa, T. Nakamura, Y. Urino, T. Fujita, "Silicon Photonics for Next Generation System Integration Platform," IEEE Communications Magazine, vol. 51, no. 3, pp. 72-77, 2013.

[9] D.E. Tamir, N.T. Shaked, P.J. Wilson, S. Dolev, "High-speed and low-power electro-optical DSP coprocessor," J. Opt. Soc. Am. A., vol. 26, no. 8, pp. A11–A20, 2009.

[10] S. Antonov, A. Vainer, V. Proklov, Y. Rezvov, "Switch multiplexer of fiber-optic channels based on multibeam acousto-optic diffraction," Applied Optics, vol. 48, no. 7, pp. C171-C181, 2009.

[11] A.Y. Lipinskii, "Synthesis of diffraction gratings within the LiNbO3 crystal," Radioengineering, KhNURE Press, Kharkiv, no. 169, pp. 343–348, 2012. (in Russian)

[12] W.T. Rhodes, "Acousto-Optic Signal Processing: Convolution and Correlation," Proc. IEEE, vol. 69, no. 1, pp. 65–79, 1981.